

Excited-state Forces within the *Ab Initio* Bethe-Salpeter Formalism

Sohrab Ismail-Beigi and Steven G. Louie

Department of Physics, University of California, Berkeley, CA 94720, and
Materials Sciences Division, Lawrence Berkeley National Laboratory, Berkeley, CA 94720

October 26, 2019

Abstract

We present a first-principles formalism for calculating excited-state forces for optically excited electronic states with the GW-Bethe Salpeter method. This advance allows for efficient computation of gradients of the excited-state Born-Oppenheimer energy, allowing for the study of relaxation, molecular dynamics, and photoluminescence of excited states. The approach is applied to study photoexcited carbon dioxide and ammonia molecules, and the calculations accurately describe the observed excitation energies and photoinduced structural deformations.

Calculation of optically excited electronic states and spectra has recently become possible within the first-principles GW-Bethe Salpeter Equation (GW-BSE) formalism [1, 2]. This opens the possibility of studying photoinduced structural changes and photoluminescence. However, within this methodology, one calculates optical properties at fixed ionic positions: barring inefficient finite-difference schemes or shrewd guesses, the direction in the multidimensional space of ionic configurations which best optimizes the geometry is unknown. The problem is of practical importance since structural changes due to optical excitation are general phenomena which cause rearrangements or dissociation in molecules and change the structure or symmetry of defects in solids. The possibility of efficient *ab initio* calculation of excited-state forces opens new doors to reliable modeling and study of such rearrangements.

To this end, we present a new formalism for calculating excited-state forces within the GW-BSE approach. We develop the theory needed for the force calculations and the approximations requisite to render computations tractable and then carry out practical studies for two molecular systems. We also compare our results to those of constrained density functional theory (CDFT) [3].

Within the *ab initio* GW-BSE approach, the ground-state electron density, total energy, forces, and mean-field single-particle states $|i\rangle$ and eigenvalues ε_i are obtained using density functional theory (DFT). We then construct the RPA dielectric function ϵ^{-1} and the screened interaction $W = \epsilon^{-1}v_c$, where v_c is the Coulomb interaction $v_c(\vec{r}, \vec{r}') = 1/|\vec{r} - \vec{r}'|$. The quasiparticle excitations are evaluated by employing the GW approximation to the self-energy given by $\Sigma = iGW$ [4]. The effective quasiparticle Hamiltonian H^{qp} is

$$\hat{H}^{qp} = \hat{T} + \hat{V}_{sc} + (\hat{\Sigma} - \hat{V}_{xc}), \quad (1)$$

where T is the kinetic operator, $V_{sc} = V_{ion} + V_H + V_{xc}$ is the sum of the ionic, Hartree, and DFT exchange-correlation potentials. Traditionally, we would solve the Dyson equation to obtain quasiparticle energies ε_i^{qp} and eigenstates $|i\rangle^{qp}$ where $\hat{H}^{qp}|i\rangle = \varepsilon_i^{qp}|i\rangle^{qp}$. The quasiparticle states $|i\rangle^{qp}$ may be written as superpositions of the DFT eigenfunctions $|j\rangle$ with coefficients determined by diagonalizing \hat{H}^{qp} . However, for optical excitation calculations the diagonalization is unnecessary since the quasiparticle calculations are only an intermediate step. We remain with the DFT basis $|i\rangle$ and simply tabulate the matrix elements $H_{ij}^{qp} \equiv \langle i|\hat{H}^{qp}|j\rangle$.

With the quasiparticle data, the optical excited state properties may be obtained by solving the Bethe-Salpeter equation. Below, we use the “standard” positive-frequency version of the BSE eigenvalue equation and restrict to static screening [2]. The BSE eigenvalue equation is

$$\sum_{c'v'} H_{cv,c'v'}^{BSE} A_{c'v'}^S = \Omega_S A_{cv}^S, \quad (2)$$

$$\text{with} \quad H_{cv,c'v'}^{BSE} = (H_{cc'}^{qp}\delta_{vv'} - H_{v'v}^{qp}\delta_{cc'}) + K_{cv,c'v'}. \quad (3)$$

Here c labels unoccupied (conduction) states and v labels occupied (valence) states, A_{cv}^S is the electron-hole amplitude for finding a quasihole in state v and a quasielectron in state c , S labels an excited state, Ω_S is the excitation energy, and H^{BSE} is the effective electron-hole Hamiltonian. The excited state energy is given by $E_S = E_0 + \Omega_S$ where E_0 is the ground state energy. The key role of the off-diagonal elements of H^{qp} in the DFT eigenbasis for accurate calculation of optical properties has been stressed before [8], which we confirm below. K is the electron-hole interaction kernel with matrix elements

$$K_{cv,c'v'} = \int c(1)^* v(2) \Xi(1234) c'(3) v'(4)^* d(1234), \quad (4)$$

where we $j(1) = \langle 1|j\rangle$ is the wave function of state $|j\rangle$. The kernel Ξ is given by

$$\Xi(1234) = -\delta(13)\delta(24)W(12) + \delta(12)\delta(34)v_c(13) \quad (5)$$

The static screening approximation means that $W = \epsilon^{-1}v_c$ uses the static dielectric function $\epsilon^{-1}(\omega=0)$ in Eq. (5). We note that the full frequency dependent $\epsilon^{-1}(\omega)$ is used in the GW quasiparticle calculations. The normalization of A_{cv}^S in Eq. (3) in theory is a complex issue involving renormalization, but for our case of static screening, the proper normalization is the usual one, $\sum_{cv} |A_{cv}^S|^2 = 1$.

The aim is to compute forces on excited states, i.e. the derivatives of E_S versus the $3N_{at}$ ionic coordinate R , denoted as $\partial_R E_S$. (N_{at} is the number of atoms in the system.) The desired derivative has two parts

$$\partial_R E_S = \partial_R E_0 + \partial_R \Omega_S.$$

Standard DFT methods provide us with the ground state derivatives $\partial_R E_0$ [6]. The BSE provides a concrete procedure for computing Ω_S from well defined quantities so we can compute $\partial_R \Omega_S$ directly. Using Eq. (3) and the normalization condition on A_{cv}^S yields

$$\partial_R \Omega_S = \sum_{cv,c'v'} A_{cv}^{S*} A_{c'v'}^S \partial_R H_{cv,c'v'}^{BSE}, \quad (6)$$

where

$$\partial_R H_{cv,c'v'}^{BSE} = \partial_R H_{cc'}^{qp}\delta_{vv'} - \partial_R H_{v'v}^{qp}\delta_{cc'} + \partial_R K_{cv,c'v'}. \quad (7)$$

The derivative $\partial_R H_{ij}^{BSE}$ contains two types of terms: those involving $\partial_R H_{ij}^{qp}$ and those involving $\partial_R K$. Below, we adopt two physical approximations to render computations tractable.

In evaluating Eq. (7), we first require the derivatives of the DFT eigenstates $\partial_R |i\rangle$. Perturbation theory provides the component of the derivative of state i along the state j is

$$P_{ji}^R \equiv \langle j | \{ \partial_R |i\rangle \} \rangle = \begin{cases} 0 & \text{if } \varepsilon_i = \varepsilon_j \\ \frac{\langle j | \partial_R \hat{V}_{sc} | i \rangle}{\varepsilon_i - \varepsilon_j} & \text{if } \varepsilon_i \neq \varepsilon_j \end{cases}, \quad (8)$$

where ε_i are the DFT eigenvalues. For $\partial_R V_{sc}$, we employ density functional perturbation theory [5]: an auxiliary quadratic functional is minimized, and at the minimum $\partial_R V_{sc}$ is easily found. We perform $3N_{at}$ minimizations for the $3N_{at}$ choices of R . Next, $\partial_R H_{ij}^{qp}$ is given by

$$\partial_R H_{ij}^{qp} = \langle i | \partial_R \hat{H}^{qp} | j \rangle + \sum_k \left[P_{ik}^{R*} H_{kj}^{qp} + H_{ik}^{qp} P_{kj}^R \right]. \quad (9)$$

Evaluating $\partial_R \hat{H}^{qp} = \partial_R \hat{V}_{sc} + \partial_R (\hat{\Sigma} - \hat{V}_{xc})$ is a burden as $\partial_R \hat{\Sigma}$ contains derivatives of the Green's function and ϵ^{-1} , both of which are prohibitive to calculate. We now choose a physical approximation: V_{sc} contains the dominant ionic, Hartree, and mean-field exchange-correlation potentials which bind solids and molecules. The weaker correction $\Sigma - V_{xc}$ consists largely of a constant ‘‘scissors-shift’’ with a weak dependence on R . Therefore, we may approximate $\partial_R \hat{H}^{qp} \cong \partial_R \hat{V}_{sc}$ in Eq. (9).

Considering terms with $\partial_R K$, Eqs. (4) and (5) provide two distinct types of derivatives: those due to changes of the DFT states $\partial_R |i\rangle$ and those due to changes of screening $\partial_R W$. For the first set, we employ

Eq. (8) and sum over intermediate states to reach convergence. For the second set, we argue, and verify below, that they are negligible. In the present GW-BSE formalism, $W = \epsilon^{-1}v_c$ where $\epsilon = I - v_c P$ and P is the polarization. Within the RPA approximation employed for ϵ , P is a function of G alone given by $P = iGG$. Therefore, in the RPA, W is only a function of G . Moreover, in deriving of the interaction kernel Ξ in Eq. (5), it is assumed that $\delta W/\delta G \cong 0$ [2]. Judging from the success and accuracy of the BSE method based on this assumption, we conclude that we may set $\partial_R W \cong 0$. Thus, we arrive at the following expression for $\partial_R K$:

$$\partial_R K_{cv,c'v'} = \sum_j \left[P_{jc}^{R*} K_{jv,c'v'} + P_{jv}^R K_{cj,c'v'} + P_{j'c'}^R K_{cv,jv'} + P_{j'v'}^{R*} K_{cv,c'j} \right]. \quad (10)$$

Taken together, Eqs. (6-10) provide us with an explicit expression for $\partial_R \Omega_S$ and hence $\partial_R E_S$. We now turn to testing the approach and verifying the accuracy of our two approximations $\partial_R H^{qp} \cong \partial_R V_{sc}$ and $\partial_R W \cong 0$. As a test case, we study the first optically excitable singlet state of carbon monoxide (CO), a molecule well characterized experimentally and with only one ionic degree of freedom R , the bond length.

We carry out density functional calculations using the plane-wave pseudopotential method within the local density approximation (LDA) [6]. We use Kleinmann-Bylander pseudopotentials with s and p projectors (p local) for C and O with cutoff radii of $r_c = 1.3$ a.u. [7] and expand the electronic states to a plane wave cutoff of 70 Ry. Our periodic supercell is a $7 \times 7 \times 7 \text{ \AA}^3$ cube. We sample the Brillouin zone at $k = 0$. We perform GW calculations using the generalized plasmon-pole model [4]. We include 600 bands in the GW calculations to converge *absolute* quasiparticle and ionization energies. In the GW-BSE computations, we truncate the Coulomb interaction beyond 3.5 \AA to avoid spurious periodic image interactions (see ref. [2] for details). With these parameters, all reported energies are converged to 0.05 eV. For comparison, we also calculate approximate excited-state properties with the constrained-LDA (CLDA) method: we occupy the LUMO with an electron taken from the HOMO and iterate to self-consistency.

Fig. 1 displays the energy of ground state (LDA) and first excited states (BSE or CLDA) of CO as a function of the bond length. Table 1 lists calculated and experimental properties of the ground state ($X^1\Sigma^+$) and excited state ($A^1\Pi$): the equilibrium bond lengths R_e , harmonic vibration frequency ω_e , ionization energy IP (for the LDA taken as the HOMO energy), and the minimum-to-minimum transition energy T_e . The ground-state DFT R_e and ω_e are in good agreement with experimental results. The LDA HOMO energy, however, lies far from the ionization energy, but the GW results remove this error. The BSE results for the transition energy T_e to the excited state agree with experiment within an error typical of the method [2] whereas the CLDA transition energy is off by 1 eV. For R_e and ω_e both the CLDA and BSE perform equally well.

We mention two important technical issues. First, off-diagonal matrix elements of H^{qp} in the DFT basis must be included: their neglect changes BSE excitation energies by ~ 0.2 eV, similar to previous findings[8]. Second, long-range electrostatic interactions give rise to an ambiguity in the vacuum level in supercell calculations and shift quasiparticle energies by a constant. In practice, by varying the supercell volume V , we find the shift proportional to $1/V$ and easily extrapolate to $V \rightarrow \infty$.

Turning to the forces, we wish to know how accurately we can compute $\partial_R E_S$ directly, i.e. the slope of the curves in Fig. 1. Fig. 2 presents the calculated forces, as formulated above, along with the “exact” forces obtained from two-point finite differences of the BSE energies. In addition, as comparisons, we also compute forces by assuming $\partial_R K = 0$ in Eq. (7), a quasiparticle-only treatment and a closest analogue to the single-particle CLDA. Both these “single-particle” methods predict equal and opposite forces for the C and O atoms, a signal that $\partial_R H^{qp} \cong \partial_R V_{sc}$ is a good physical approximation. Interestingly, both methods produce very similar forces that depart from the “exact” forces by essentially a constant. Hence, although these single-particle approaches do not yield the correct force, they can predict the variation of the force versus bond length quite well, an *a posteriori* verification of our physical approximation that changes in the mean-field potentials dominate.

When we include contributions from $\partial_R K$, the calculated forces improve markedly. Since we assume that $\partial_R W \cong 0$, the forces on C and O are no longer exactly equal and opposite. However, as Fig. 2 shows, the deviations are quite small on the relevant scale: as we argued above, the approximation $\partial_R W \cong 0$ is

excellent in practice. When we subtract the unphysical net force on the center of mass, which amounts to a force value halfway between the C and O values in Fig. 2, the calculated force become essentially “exact”.

Carbon monoxide has a single ionic degree of freedom which allows for a careful study. However, calculation of forces is truly useful when there are many ionic degrees of freedom and one does not know, *a priori*, which are the relevant ones for a given excited state. Thus, as a more complex example, we consider the first optically excitable singlet state of ammonia, NH_3 , a system with twelve degrees of freedom. An identical methodology is employed to the case of CO above and we mention relevant parameters. The hydrogen pseudopotential has an s projector with $r_c=0.8$ a.u. and the nitrogen has s and p projectors (p local) with $r_c=1.0$ a.u. We use the same supercell, k-point sampling, and Coulomb truncation radius listed above. We use a 50 Ry cutoff for the DFT wave functions and 600 bands to calculate ϵ and quasiparticle energies. All energies are converged to 0.05 eV.

Table 2 lists key properties of the ground-state structure within the LDA. Starting with this ground-state structure, for the BSE we consider the first excited state, and for the CLDA we promote an electron from HOMO to LUMO. We calculate excited state forces and perform relaxations until the structure is converged to 0.01 Å in bond lengths R_e , 1° in bond angle θ , and 0.01 eV in transition energies T_e (typically requiring 6 iterations). Table 2 presents results for the relaxed excited states. Experimentally, the first excited state is known to possess a planar geometry with elongated bonds [10] which is precisely what we find. As expected, the BSE excitation energy compares well with the experimental value. In addition, as in the case of CO, the CLDA and BSE give equally good optimized geometries for the excited state (the excellent agreement with experiment for the bond length is likely fortuitous).

Based on the two cases of CO and NH_3 , we verify the accuracy of the BSE method for calculation of excited state energies and geometries. Our approach provides excited-state forces which are, to an excellent approximation, the derivatives of the BSE energies. Intriguingly, for these two cases, while CDFT yields inferior excitation energies, its predicted structural relaxations are of comparable quality to the BSE ones. While encouraging, there are a number of serious problems with wider use of CDFT. Use of CDFT is straightforward when the excited state is composed mainly of a single configuration (for the first excited states of CO and NH_3 , the HOMO-LUMO combination had weight in excess of 90%). However, for higher excited states, we find that multiple configurations are needed, something we can not know without performing the BSE calculation. In addition, for higher excited states within CDFT, the self-consistent calculations were *unstable* and could not be converged. Finally, CDFT, a single-particle theory and subject to Koopman’s theorem, fails completely at describing excitonic binding in extended solids. For all these reasons, we believe that while CDFT may be useful as a guide in some particular circumstances, the results thus obtained should be carefully tested by more sophisticated methods.

In summary, we present our *ab initio* formalism for calculation of excited-state forces within the GW-BSE method as well as approximations allowing for computational tractability. We calculated the photoexcited properties of two molecules and verified the accuracy of (a) the GW-BSE formalism for describing the excited-state energetics and structural relaxations, and (b) the forces used for the relaxations as calculated by our formalism.

This work was supported by National Science Foundation (NSF) grant #DMR-0087088 and by the Office of Energy Research, Office of Basic Energy Sciences, Materials Science Division of the U.S. Department of Energy (DOE) contract #DE-AC03-76SF00098. Computer resources were provided by the DOE at the Lawrence Berkeley National Laboratory National Energy Research Scientific Computing Center and by the NSF National Partnership for Advanced Computational Infrastructure at the San Diego Supercomputing Center. Support from the DOE Computational Materials Science Network is also gratefully acknowledged.

References

- [1] M. Rohlfing and S. G. Louie, Phys. Rev. Lett.**81** 2312 (1998); S. Albrecht, L. Reining, R. Del Sole, and G. Onida, Phys. Rev. Lett.**80**, 4510 (1998); L. X. Benedict, E. L. Shirley, and R. B. Bohn, Phys. Rev. Lett.**80**, 4514 (1998).
- [2] M. Rohlfing and S. G. Louie, Phys. Rev. B**62**, 4927 (2000).
- [3] F. Mauri and R. Car, Phys. Rev. Lett.**75** 3166 (1995).

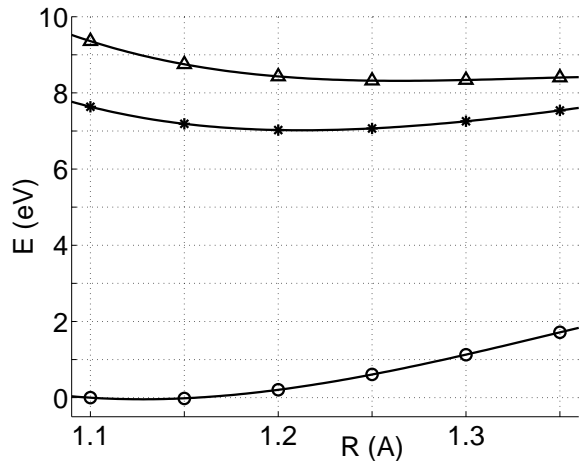


Figure 1: $X^1\Sigma^+$ ground state (circles) and $A^1\Pi$ first excited state (triangles and stars) energies for CO versus the bond length R . The triangles are the GW-BSE results and the stars are the CLDA results. The continuous curves are polynomial fits to guide the eye.

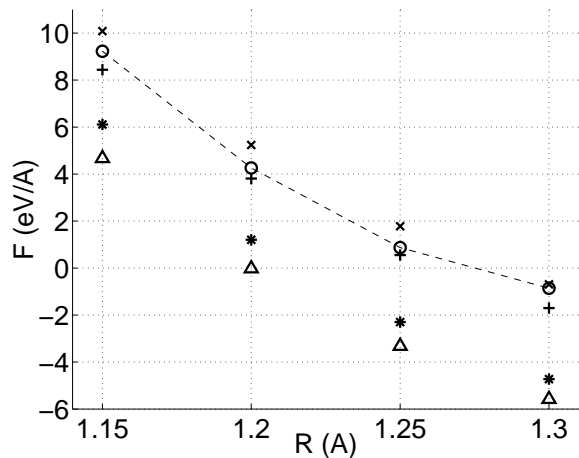


Figure 2: Absolute magnitudes of $A^1\Pi$ excited state forces for CO. Circles are “exact” GW-BSE forces, crosses and pluses are GW-BSE forces on C and O, triangles are GW-BSE forces with $\partial_R K = 0$, and stars are CLDA forces. The dashed curve is meant as a guide to the “exact” results.

Ground state ($X^1\Sigma^+$)	R_e (Å)	ω_e (cm^{-1})	IP (eV)
LDA	1.13	2050	9.1
GW	–	–	14.1
Expt. [9]	1.1283	2169.8	14.01
Excited state ($A^1\Pi$)	R_e (Å)	ω_e (cm^{-1})	T_e (eV)
CLDA	1.21	1720	7.02
GW-BSE	1.26	1290	8.32
Expt. [9]	1.235	1518.2	8.07

Table 1: Ground state and first excited state data for carbon monoxide: equilibrium bond length R_e , harmonic vibrational frequency ω_e , ionization potential IP , and $X^1\Sigma^+ \rightarrow A^1\Pi$ transition energy T_e .

Ground state (\tilde{X}^1A_1)	R_e (Å)	θ ($^\circ$)	IP (eV)
LDA	1.03	105.0	6.2
GW	–	–	10.7
Expt. [9, 10]	1.01	106.7	10.1

Excited state (\tilde{A}^1A_2'')	R_e (Å)	θ ($^\circ$)	T_e (eV)
CLDA	1.08	120	5.05
GW-BSE	1.08	120	5.52
Expt. [10]	1.08	120	5.7

Table 2: Ground state and first excited state data for NH_3 : equilibrium bond length R_e , H-N-H angle θ , ionization potential IP , and $\tilde{X}^1A_1 \rightarrow \tilde{A}^1A_2''$ transition energy T_e . The experimental T_e contains a zero-point contribution of small but unknown size.

- [4] M. S. Hybertsen and S. G. Louie, *Phys. Rev.* **B34** 5390 (1986).
- [5] X. Gonze, D. C. Allan and M. P. Teter, *Phys. Rev. Lett.* **68** 3603 (1992).
- [6] M. C. Payne, M. P. Teter, D. C. Allan, T. A. Arias, and J. D. Joannopoulos, *Rev. Mod. Phys.* **64**, 1045 (1992), and references therein.
- [7] L. Kleinman and D. M. Bylander, *Phys. Rev. Lett.* **48**, 1425 (1982).
- [8] J. C. Grossman, M. Rohlfing, L. Mitas, S. G. Louie, and M. L. Cohen, *Phys. Rev. Lett.* **86**, 472 (2001).
- [9] *NIST Chemistry WebBook, NIST Standard Reference Database #69*, Eds. P.J. Linstrom and W.G. Mallard, July 2001 (<http://webbook.nist.gov>).
- [10] G. Herzberg, *Electronic Spectra and Electronic Structure of Polyatomic Molecules*, New York: Krieger, 1991.